ChemComm

COMMUNICATION

View Article Online
View Journal | View Issue

Cite this: *Chem. Commun.*, 2017, 53, 11161

Received 4th July 2017,
Accepted 1st September 2017

DOI: 10.1039/c7cc05166b

rsc.li/chemcomm

Lysosomal tracking with a cationic naphthalimide using multiphoton fluorescence lifetime imaging microscopy†

Meng Li,‡*[ab] Haobo Ge,‡*[a] Vincenzo Mirabello,[a] Rory L. Arrowsmith,[a] Gabriele Kociok-Köhn,[a] Stanley W. Botchway,[c] Weihong Zhu,*[d] Sofia I. Pascu*[a] and Tony D. James*[a]

A naphthalimide-based chemosensing motif turns ON the fluorescence emission in solution in the presence of aqueous iron(III) chloride, and maintains this property in living cancer cells. The emission response to Fe(III) ions occurs simultaneously with a change in pH. The protonation of methyl piperazine-conjugated naphthalimide promotes its lysosomal localisation as assessed by co-localisation tests and fluorescence lifetime imaging microscopy (FLIM) *in vitro*.

The development of highly sensitive and selective probes for the recognition and measurement of transition metal ions *in vitro* are necessary tools in biological,[1,2] chemical[3–5] and environmental science.[6–9] Iron is one of the essential metal ions in biological systems since it plays a fundamental role in many biochemical processes.[7,10–15] Both its deficiency and overload may lead to biological disorders *in vivo*, such as anaemia, liver and kidney damage, heart failure and diabetes onset.[16–18] Due to its biological significance, fluorescence probes for the precise detection of iron(III) are sought after.[19–23] Since in aqueous conditions at neutral pH, Fe(III) halides form insoluble $Fe(OH)_3$ and, in the lysosomes (pH 4.5), species such as $[Fe(OH)_2]^+$ and $[Fe(OH)]^{2+}$ with release of protons,[24] there are only a few Fe^{3+} fluorescent sensors that can directly detect this ion, especially with turn-on fluorescence response.[25–27] It is generally accepted that simple and effective chemosensors that involve fluorescence turn-on are advantageous.[28,29] By using a "turn on" probe, it is possible to measure low-concentrations because measuring a small increase relative to a dark background, reduces the likelihood of false positive signals and increases sensitivity.[30,31] Therefore, we aimed to design and deliver to cells a biocompatible fluorescent probe that turns into a highly fluorescent, protonated species, only in the presence of trivalent cations such as Fe(III) *in vitro*. We also investigated the effect of an excess of aqueous tricationic chlorides resembling the Fe(III) charge and size ratios and the coupled pH variation caused on a simple naphthalimide-based fluorescent probe tagged with a Lewis base methyl piperazine as the receptor of choice. Photo-induced electron transfer (PET) chemosensors with the 'fluorophore-spacer-receptor' format, are one of the most important classes for the design of fluorescent sensors.[32] Naphthalamide was the fluorophore tag of choice due to its excellent photophysical properties, including high extinction coefficient, photostability and relatively long emission wavelength (500–600 nm).[33,34] The intermediate **TN** was first synthesised from 4-bromo-1,8-naphthalic anhydride and 5-methylthiazol-2-amine by refluxing in absolute acetic acid (60% yield, ESI,† Scheme S1). The bromine atom of **TN** was then substituted by methyl-piperazine in 2-methoxyethanol

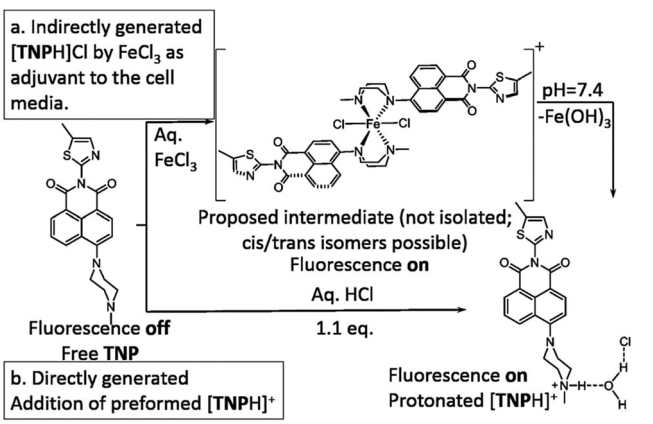

Scheme 1 Proposed pathway for the **TNP** protonation leading to the fluorescent [**TNP**H]Cl *in situ* in aqueous $FeCl_3$ media.

[a] *Department of Chemistry, University of Bath, Claverton Down, Bath, BA2 7AY, UK. E-mail: t.d.james@bath.ac.uk, s.pascu@bath.ac.uk*
[b] *Department of Environmental Science and Engineering, North China Electric Power University, 689 Huadian Road, Baoding, 071003, P. R. China. E-mail: mli201509@163.com*
[c] *Central Laser Facility, Rutherford Appleton Laboratory, Research Complex at Harwell, STFC Didcot, OX11 0QX, UK*
[d] *Shanghai Key Laboratory of Functional Materials Chemistry, Key Laboratory for Advanced Materials and Institute of Fine Chemicals, East China University of Science & Technology, Shanghai 200237, P. R. China. E-mail: whzhu@ecust.edu.cn*

† Electronic supplementary information (ESI) available: Syntheses, spectroscopy, ESI-MS, NMR, X-ray crystal data, cell culture, confocal and fluorescence lifetime data. CCDC 1542385. For ESI and crystallographic data in CIF or other electronic format see DOI: 10.1039/c7cc05166b

‡ These authors contributed equally to the work.

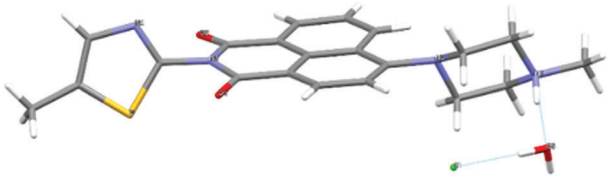

Fig. 1 Molecular structure of [**TNP**H]Cl·H_2O by single crystal X-ray diffraction. Crystals were grown from a mixture of 2 : 1 TNP and $FeCl_3$ in wet DMSO. Colour code: yellow: sulfur, red: oxygen, grey: carbon, light grey: hydrogen, green: chlorine. Details are given in the ESI† and Fig. S13, S14.

yielding **TNP**, which was treated with either an excess of aqueous $FeCl_3$ or HCl to give [**TNP**H]$^+$ species (Scheme 1). The coordination chemistry of $FeCl_3$ with various modifications of *N*-aryl or *N*-alkyl-piperazine ligands has been reported.[35,36] When coordinated to the Fe^{3+} metal centre, the ligand likely adopts a boat configuration acting as a bidentate chelator, however the [(**TNP**)$_2$$FeCl_2$]$^+$ intermediate proposed in Scheme 1 (on the basis of mass spectrometry) could not be isolated on a laboratory scale from wet solvents used for the sensing and imaging experiments as it rapidly decomposed to form [**TNP**H]Cl (*vide infra*). This new compound was fully characterized by ^{1}H and ^{13}C NMR spectroscopies, HRMS, and single crystal X-ray diffraction (Fig. 1 and ESI†). The photo-physical properties of the free **TNP** were investigated using UV-vis absorption and fluorescence spectroscopies including titration studies with aqueous $FeCl_3$ under an aqueous environment (Fig. S1 and S6, ESI†). In HEPES buffer, free **TNP** showed one main absorption band centred at 410 nm (ε = 1.3 × 10^4 M^{-1} cm^{-1}) assigned as a π–π* transition (10 mM HEPES; ethanol/H_2O = 80 : 20, v/v; pH 7.4, Fig. S1, ESI†).

Upon the addition of Fe^{3+} (0–10 eq. $FeCl_3$), the maximum absorption peak exhibits a distinct shift from 410 to 381 nm. When excited in the proximity of its isosbestic point (403 nm in single-photon, or 810 nm in two-photon mode), **TNP** shows only weak fluorescence emission due to PET. In the presence of $FeCl_3$, in a variety of (wet) organic solvents, a strong fluorescence emission with a maximum at 515 nm was observed, as shown in Fig. 2. Furthermore, the fluorescence intensities at 515 nm display a nonlinear relationship towards Fe^{3+} concentrations from 0.2 to 10 μM, and the binding constant is (3.75 ± 0.31) × 10^5 M^{-1}, indicating that **TNP** is particularly sensitive to the detection of Fe^{3+} (ESI,† Fig. S6). An intense peak at *m*/*z* 910.1347 in the electron-spray MS ionization (ESI) exhibited the correct isotopic pattern corresponding to the species [**TNP**$FeCl_2$]$^+$ and also several related fragments indicative of the formation of an [**TNP**] : [iron] complex with a 2 : 1 stoichiometry (Scheme 1 and ESI,† Fig. S4). The selectivity of **TNP** toward Lewis acids such as Fe^{3+}, Cr^{3+}, Al^{3+} was evaluated by adding 10 eq. of various metal ions, including those essential ions of relevance to biological processes *in vivo* (Cu^{2+}, Co^{2+}, Ni^{2+}, Fe^{2+}, Na^+, K^+, Ca^{2+} and Mg^{2+}) and toxic metals such as Hg^{2+}, Cd^{2+}, Pd^{2+}, Ag^+. Under the same conditions, no obvious fluorescence changes were observed for the M^{2+} ions tested (Fig. 2b). A Job's plot analysis indicated that the binding mode of **TNP** donors to Fe^{3+} was 2 : 1 (ESI,† Fig. S3). **TNP** is therefore very selective and sensitive for aqueous Fe^{3+} which is essential to life as well as being earth abundant, and we hypothesised that this is due to the initial formation of the corresponding metal complex. In the case of aqueous $FeCl_3$ (Scheme 1) this was followed by its decomposition to [**TNP**H]Cl in

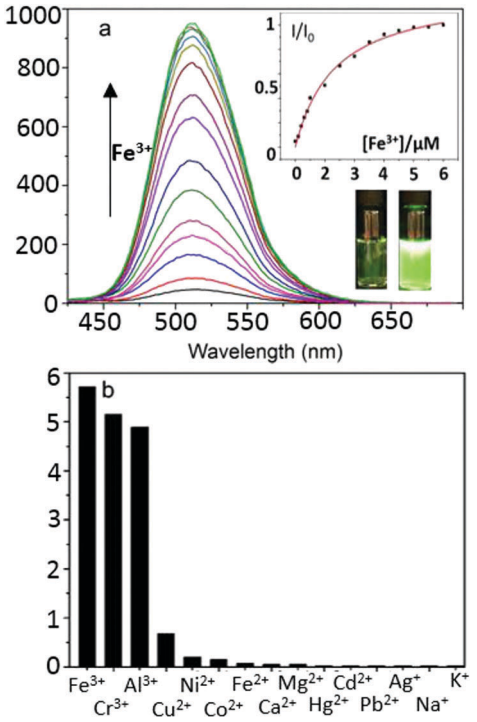

Fig. 2 (a) Steady-state single photon fluorescence spectroscopy (λ_{ex} = 403 nm) of **TNP** (1 μM) in ethanol–water (80 : 20, v/v) with a buffer solution of HEPES (10 mM, pH = 7.4) in the presence of different concentrations of aqueous metal ions. Inset: Fluorescence intensity at 515 nm of **TNP** as a function of aqueous Fe^{3+} concentration. (b) Fluorescence intensity change of **TNP** (1 μM) in the presence of metal ions (10 μM).

the wet solvents used (ESI†). [**TNP**H]Cl was also isolated by reacting **TNP** with 1.1 eq. of concentrated HCl (Scheme 1). The quantum yield of [**TNP**H]Cl in DMSO was measured to be 0.017, comparable with other naphtyl-based chromophores (ESI†). Taken together, data suggests that the initial capture of Fe^{3+} by the receptor results in a decrease of the electron-donating ability of the methyl-nitrogen, thus resulting in a reduction of the PET effect, and with time, (in the presence of H_2O) in the formation of the protonated species [**TNP**H]Cl (as well as presumably [$Fe(H_2O)_3(OH)_3$] and $Fe(OH)_3$ and aqueous HCl). The protonated species could well form under differing condition too: specimens with the same unit cell parameters were isolated and characterised by X-ray diffraction from several different aqueous solvent mixtures (EtOH/H_2O, DMSO, wet $CHCl_3$) (Fig. 1 and ESI†). The onset of enhanced fluorescence upon treatment with an excess of aqueous $FeCl_3$ was also observed in experiments carried out using 2-photon excitation in wet DMSO for steady-state emission spectra and excited state lifetime measurements. While the fluorescence emissions were remarkably different (ESI†), lifetime measurement *via* time correlated single photon counting (TCSPC) indicated that the lifetime point decays recorded in solutions (giving rise to data which was modelled to 1 component multi-exponential fitting) are in the region of *ca.* 5 ns for both [**TNP**] and [**TNP**H]Cl (the latter being generated *in situ*, from the **TNP** in the presence of excess $FeCl_3$ in wet DMSO). Specifically, free [**TNP**] in solution showed a 4.92 ns (χ^2 = 1.28) and, in the presence of aqueous $FeCl_3$ (*in situ* protonation) giving rise to the protonated species [**TNP**H]$^+$ increased to 5.56 ns (χ^2 = 1.19)

(ESI,† Fig. S24–S26). These results confirmed the iron-mediated protonation of methyl piperazine unit disrupts the PET turning on the fluorescence of the probe. Studies of the pH-dependent response of **TNP** were also carried out over a pH range of 3.0–9.0 (ESI,† Fig. S7). We explored the ability of **TNP** towards *in vitro* conversion to [**TNP**H]$^+$ in the acid environment of lysosomes. The cellular environment of the new probe was determined in HeLa and PC-3 cancer cells using confocal fluorescence spectroscopy and fluorescence lifetime imaging microscopy (FLIM) (Fig. S27 and S28, ESI†), which is used as a sensitive analytical tool for the probes' environment with added advantages when using multiphoton imaging techniques, *i.e.* the use of tissue-friendly low energy near infra-red photon rather than UV excitation for live cells. The pH evaluation showed that between pH 7.4–9.0 (well within the biologically relevant pH range 6.5–8.5) the emission of free **TNP** is turned off in aqueous solutions. On the contrary, at lower pH, [**TNP**H]Cl, a highly fluorescent and kinetically stable organic molecule, was formed. This new lipophilic cation may be employed further to measure pH changes. However, such sensing experiments are beyond the scope of this study. Cells were incubated at 37 °C with **TNP** and visualised using single photon, epi- and confocal-fluorescence microscopies (Fig. 3 and ESI†) and two-photon confocal fluorescence microscopy coupled with fluorescence lifetime imaging microscopy (FLIM Fig. 4 and ESI.† Cellular assays were prepared according to standard methods:[9,34,37–41] generally, cells were incubated with **TNP** in the presence or absence of $FeCl_3$ as well as with [**TNP**H]Cl solutions for 15 minutes in serum free medium (SFM). After washing with PBS, the cells were imaged using laser scanning confocal fluorescence microscopy (in single- or two-photon excitation modes). Control experiments (Fig. S15 and S16, ESI†) were carried out in cells incubated with serum free medium alone, or with 1 to 2% DMSO in SFM). The confocal imaging results regarding the iron-mediated fluorescence enhancement in cells were most promising using an excitation wavelength of 405 nm (single-photon excitation) or 810 nm (under two-photon excitation). The imaging studies also indicated that **TNP** alone passes through cell membranes but its fluorescence is extremely weak. Single-photon, as well as two-photon microscopy experiments, were repeated in a PC-3 (a prostate cancer cell line), also incubated at 37 °C (ESI†). In both HeLa and PC-3, in the presence of an excess of aqueous $FeCl_3$ (minimum 1 mM concentration), the characteristic and intense fluorescence emission and the corresponding lifetime of [**TNP**H]$^+$ can be reliably observed away from that of cellular auto fluorescence. The experiments carried out at 4 °C did not show reliable uptake of **TNP**, either alone or in the presence of $FeCl_3$. Imaging experiments of **TNP** alone with incubation times longer than 1 h or at concentrations higher than 100 μM (with 1–2% DMSO) did not show reliable results due to the lack of fluorescence emission and were not pursued. The ability of [**TNP**H]$^+$ to localise in the acidic intracellular organelles *in vitro* was investigated in both HeLa and PC-3 cells using 1P- and 2P-confocal fluorescence microscopies and FLIM. Co-localisation studies were carried out using LysoTracker Red CMXRos, and confirm the ability of [**TNP**H]$^+$ to target the acidic organelles and be co-localised in the lysosomes (Fig. 5 and ESI†). Control experiments were carried out on cells incubated with DMSO and **TNP** alone (10 μM) at various temperatures and compared with probe-free control experiments in cells (incubated with SFM, or with 1 to 2% DMSO in SFM). In conclusion, imaging experiments in cancer cells reliably showed that a strong fluorescence emission is detectable for TNP only when this is converted to [TNPH]$^+$: we call this acido-modulation of the fluorescence response of a Lewis base in cells. Imaging experiments in cancer cells suggested that a strong fluorescence emission is detectable for the protonated species **TNP**H$^+$ in the presence of iron(III) at moderate concentrations (50 μM), within a comparable order of magnitude with that of commercial chemosensors based on chelators, and of relevance to the detection of free ion on concentration scales, of *ca.* 18 μM in plasma ion concentrations.

In conclusion, we showed the dual capability of the naphthalimide-based probe in the sensitive detection Fe(III) *in vitro*, and its application in the selective visualization of the acidic lysosomes using FLIM. This highlights the potential of **TNP** as a chemosensor for lysosomal tracking, confirmed by co-localisation tests. Further studies are in progress to identify the likely cytotoxicity: ESI† gives initial MTT tests in a range of cells and conditions. Our ongoing interest is to establish a

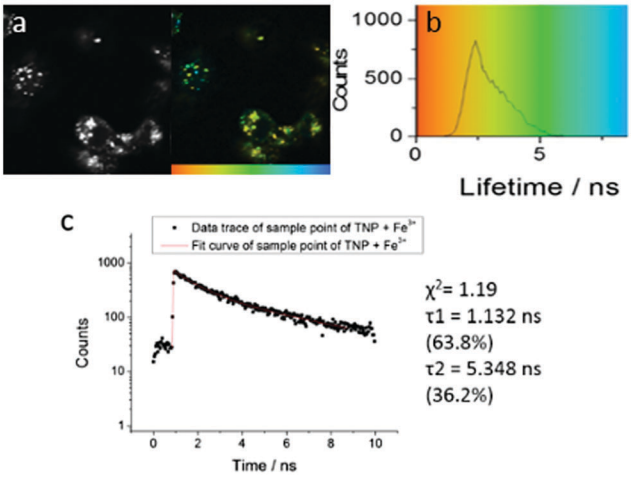

Fig. 4 Two-photon FLIM of **TNP**HCl (showing the same cluster of HeLa cells as above, albeit with slightly shifted field of view due to instrument alignment) formed from **TNP** in the presence of excess aqueous $FeCl_3$ (37 °C, 50 μM, 1% DMSO, 15 minutes incubation, 1% DMSO of **TNP**, 5 eq. $FeCl_3$). Images show: (a) 2P fluorescence lifetime FLIM map (λ_{ex} = 810 nm); (b) corresponding lifetime distribution curve (ns) showing an average lifetime distribution (τ_m) of 2.40 ± 1.25 ns, (c). A representative point decay trace corresponding to the blue cursor whereby the value of the τ_2 component (*ca.* 5 ns, similar to the lifetime of free **TNP** in solution) is suggestive of a **TNP** core present within the lysosomal cells' regions (ESI†).

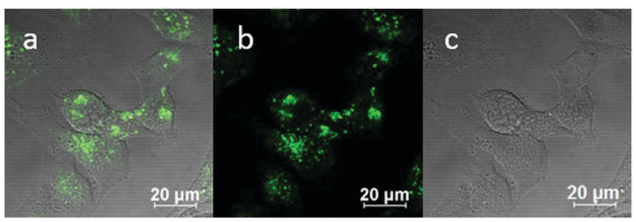

Fig. 3 Single photon confocal fluorescence imaging of [**TNP**H]Cl formed *in situ* in aqueous media (a–c) in HeLa cells (37 °C, 50 μM, 1% wet DMSO, 15 minutes incubation of TNP, 1% wet DMSO, DMEM containing 5 eq. of $FeCl_3$). (a) Overlaid images of fluorescence emission channels with DIC channel, (b): excitation wavelength: 405 nm, and long-pass filtered at 515 nm; (c and f): DIC images. Scale bar = 20 μm.

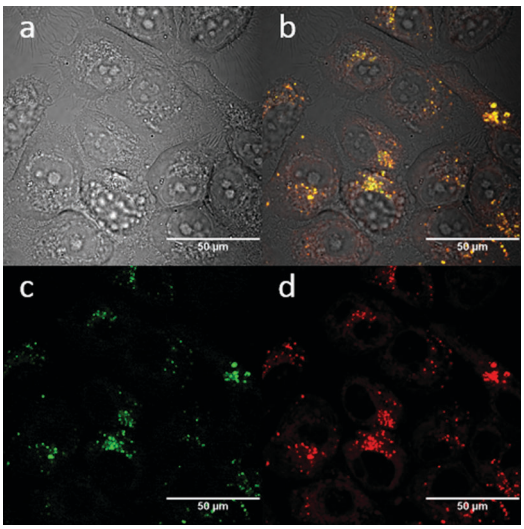

Fig. 5 Confocal fluorescence imaging of [**TNP**H]$^+$ in PC3 cells (37 °C, 15 minutes incubation, 10 mM 1 : 99 in cell media, λ_{ex} = 488 nm). Cells were pre-incubated with lysosome red tracker (1 μM 1 : 99 in cell media, 30 minutes incubation at 37 °C). (a) DIC channel; (b) overlay of the blue-green-red channels; (c) green channel (λ_{em} = 500–550 nm); (d) red channel (λ_{em} = 570–750 nm). Scale bar: 50 μm.

trend for **TNP** behaviour in the presence of other trivalent ions *e.g.* of relevance to molecular imaging *in vivo* such as ^{67}Ga or ^{68}Ga species for nuclear medicine as diagnostics, as these would likely mimic the behaviour of trivalent iron. The responsiveness of **TNP** upon protonation within intracellular compartments as well as in tumour micro-environments are our ongoing investigations.

S. I. P. is grateful to the EC for the ERC Consolidator fellowship O2SENSE (617107). T. D. J. and S. I. P. thank the Royal Society for funding. T. D. J. thanks ECUST for a Guest Professorship. T. D. J. and M. L. are grateful for financial support from China Scholarship Council (CSC) and University of Bath Full Fees Scholarship. The Catalysis and Sensing for our Environment (CASE) network is thanked for research exchange opportunities. W. H. Z. is grateful for financial support from the Oriental Scholarship and the Fundamental Research Funds for the Central Universities (WK1013002). M. L. thanks the NSF of China (21607044), NSF of Hebei Province (B2017502069) and Fundamental Research Funds for the Central Universities (2016MS108). SWB acknowledges Laserlab-Europe EU-H2020 654148. We thank Yue Wu (ECUST) for contributions in preliminary stages. We thank the EPSRC Mass spectrometry (Swansea) and the National X-ray Crystallography (Southampton) Services.

Conflicts of interest

There are no conflicts to declare.

Notes and references

1 M. Zhou, Z. Zhou, A. Gong, Y. Zhang and Q. Li, *Talanta*, 2015, **143**, 107–113.
2 B. Sui, S. Tang, T. Liu, B. Kim and K. D. Belfield, *ACS Appl. Mater. Interfaces*, 2014, **6**, 18408–18412.
3 B.-Y. Chen, C.-C. Kuo, Y.-S. Huang, S.-T. Lu, F.-C. Liang and D.-H. Jiang, *ACS Appl. Mater. Interfaces*, 2015, **7**, 2797–2808.
4 G. Mun, S. H. Jung, A. Ahn, S. S. Lee, M. Y. Choi, D. H. Kim, J.-Y. Kim and J. H. Jung, *RSC Adv.*, 2016, **6**, 53912–53918.
5 K. Zheng, K. L. Lou, C. H. Zeng, S. S. Li, Z. W. Nie and S. Zhong, *J. Photochem. Photobiol.*, 2015, **91**, 814–818.
6 Q. Zou, X. Li, J. Zhang, J. Zhou, B. Sun and H. Tian, *Chem. Commun.*, 2012, **48**, 2095–2097.
7 Z.-Q. Guo, W.-Q. Chen and X.-M. Duan, *Org. Lett.*, 2010, **12**, 2202–2205.
8 Y. Ma, W. Luo, P. J. Quinn, Z. Liu and R. C. Hider, *J. Med. Chem.*, 2004, **47**, 6349–6362.
9 M. Li, H. Ge, R. L. Arrowsmith, V. Mirabello, S. W. Botchway, W. Zhu, S. I. Pascu and T. D. James, *Chem. Commun.*, 2014, **50**, 11806–11809.
10 D. W. Domaille, E. L. Que and C. J. Chang, *Nat. Chem. Biol.*, 2008, **4**, 168–175.
11 D. Buccella, J. A. Horowitz and S. J. Lippard, *J. Am. Chem. Soc.*, 2011, **133**, 4101–4114.
12 P. A. Gale, S. E. García-Garrido and J. Garric, *Chem. Soc. Rev.*, 2008, **37**, 151–190.
13 D. R. Richardson and P. Ponka, *Biochim. Biophys. Acta*, 1997, **1331**, 1–40.
14 E. L. Mackenzie, K. Iwasaki and Y. Tsuji, *Antioxid. Redox Signaling*, 2008, **10**, 997–1030.
15 Q. Zhao, F. Li and C. Huang, *Chem. Soc. Rev.*, 2010, **39**, 3007–3030.
16 F. Bousejra-ElGarah, C. Bijani, Y. Coppel, P. Faller and C. Hureau, *Inorg. Chem.*, 2011, **50**, 9024–9030.
17 J. Morrissey and M. L. Guerinot, *Chem. Rev.*, 2009, **109**, 4553–4567.
18 L. A. Ba, M. Doering, T. Burkholz and C. Jacob, *Metallomics*, 2009, **1**, 292–311.
19 J. Huang, Y. Xu and X. Qian, *Org. Biomol. Chem.*, 2009, **7**, 1299–1303.
20 R. K. Jackson, Y. Shi, X. Yao and S. C. Burdette, *Dalton Trans.*, 2010, **39**, 4155–4161.
21 E. L. Que, D. W. Domaille and C. J. Chang, *Chem. Rev.*, 2008, **108**, 1517–1549.
22 J. Cao, C. Zhao, X. Wang, Y. Zhang and W. Zhu, *Chem. Commun.*, 2012, **48**, 9897–9899.
23 Y. Wei, Z. Aydin, Y. Zhang, Z. Liu and M. Guo, *ChemBioChem*, 2012, **13**, 1569–1573.
24 D. Ghernaout, A. I. Al-Ghonamy, A. Boucherit, B. Ghernaout, M. W. Naceur, N. A. Messaoudene, M. Aichouni, A. A. Mahjoubi and N. A. Elboughdiri, *Am. J. Environ. Prot.*, 2015, **4**, 1–15.
25 R. Wang, F. Yu, P. Liu and L. Chen, *Chem. Commun.*, 2012, **48**, 5310–5312.
26 B. Wang, J. Hai, Z. Liu, Q. Wang, Z. Yang and S. Sun, *Angew. Chem., Int. Ed.*, 2010, **49**, 4576–4579.
27 Z.-Q. Hu, X.-M. Wang, Y.-C. Feng, L. Ding, M. Li and C.-S. Lin, *Chem. Commun.*, 2011, **47**, 1622–1624.
28 T. Ueno and T. Nagano, *Nat. Methods*, 2011, **8**, 642–645.
29 H. Weizman, O. Ardon, B. Mester, J. Libman, O. Dwir, Y. Hadar, Y. Chen and A. Shanzer, *J. Am. Chem. Soc.*, 1996, **118**, 12368–12375.
30 K. Rurack, M. Kollmannsberger, U. Resch-Genger and J. Daub, *J. Am. Chem. Soc.*, 2000, **122**, 968–969.
31 Y. Liu, Y. Liu, Z. Xu, L. Yang, Z. Wang, D. Zhang and Y. Ye, *Monatshefte für Chemie-Chemical Monthly*, 2016, **147**, 311–317.
32 Y. Xiao and X. Qian, *Tetrahedron Lett.*, 2003, **44**, 2087–2091.
33 J. J. P. Desvergne and A. W. Czarnik, *Chemosensors of ion and molecule recognition*, Springer, 1997.
34 S.-Y. Xu, X. Sun, H. Ge, R. L. Arrowsmith, J. S. Fossey, S. I. Pascu, Y.-B. Jiang and T. D. James, *Org. Biomol. Chem.*, 2015, **13**, 4143–4148.
35 M. Ostermeier, C. Limberg and B. Ziemer, *Z. Anorg. Allg. Chem.*, 2006, **632**, 1287–1292.
36 A. Marzotto, D. A. Clemente and G. Valle, *Acta Crystallogr., Sect. C: Cryst. Struct. Commun.*, 1999, **55**, 43–46.
37 Z. Hu, G. D. Pantoş, N. Kuganathan, R. L. Arrowsmith, R. M. Jacobs, G. Kociok-Köhn, J. O'Byrne, K. Jurkschat, P. Burgos and R. M. Tyrrell, *Adv. Funct. Mater.*, 2012, **22**, 503–518.
38 S. I. Pascu, P. A. Waghorn, T. D. Conry, B. Lin, H. M. Betts, J. R. Dilworth, R. B. Sim, G. C. Churchill, F. I. Aigbirhio and J. E. Warren, *Dalton Trans.*, 2008, 2107–2110.
39 S. I. Pascu, P. A. Waghorn, B. W. Kennedy, R. L. Arrowsmith, S. R. Bayly, J. R. Dilworth, M. Christlieb, R. M. Tyrrell, J. Zhong and R. M. Kowalczyk, *Chem. – Asian J.*, 2010, **5**, 506–519.
40 I. S. Alam, R. L. Arrowsmith, F. Cortezon-Tamarit, F. Twyman, G. Kociok-Köhn, S. W. Botchway, J. R. Dilworth, L. Carroll, E. O. Aboagye and S. I. Pascu, *Dalton Trans.*, 2015, **45**, 144–155.
41 P. A. Waghorn, M. W. Jones, M. B. Theobald, R. L. Arrowsmith, S. I. Pascu, S. W. Botchway, S. Faulkner and J. R. Dilworth, *Chem. Sci.*, 2013, **4**, 1430–1441.

